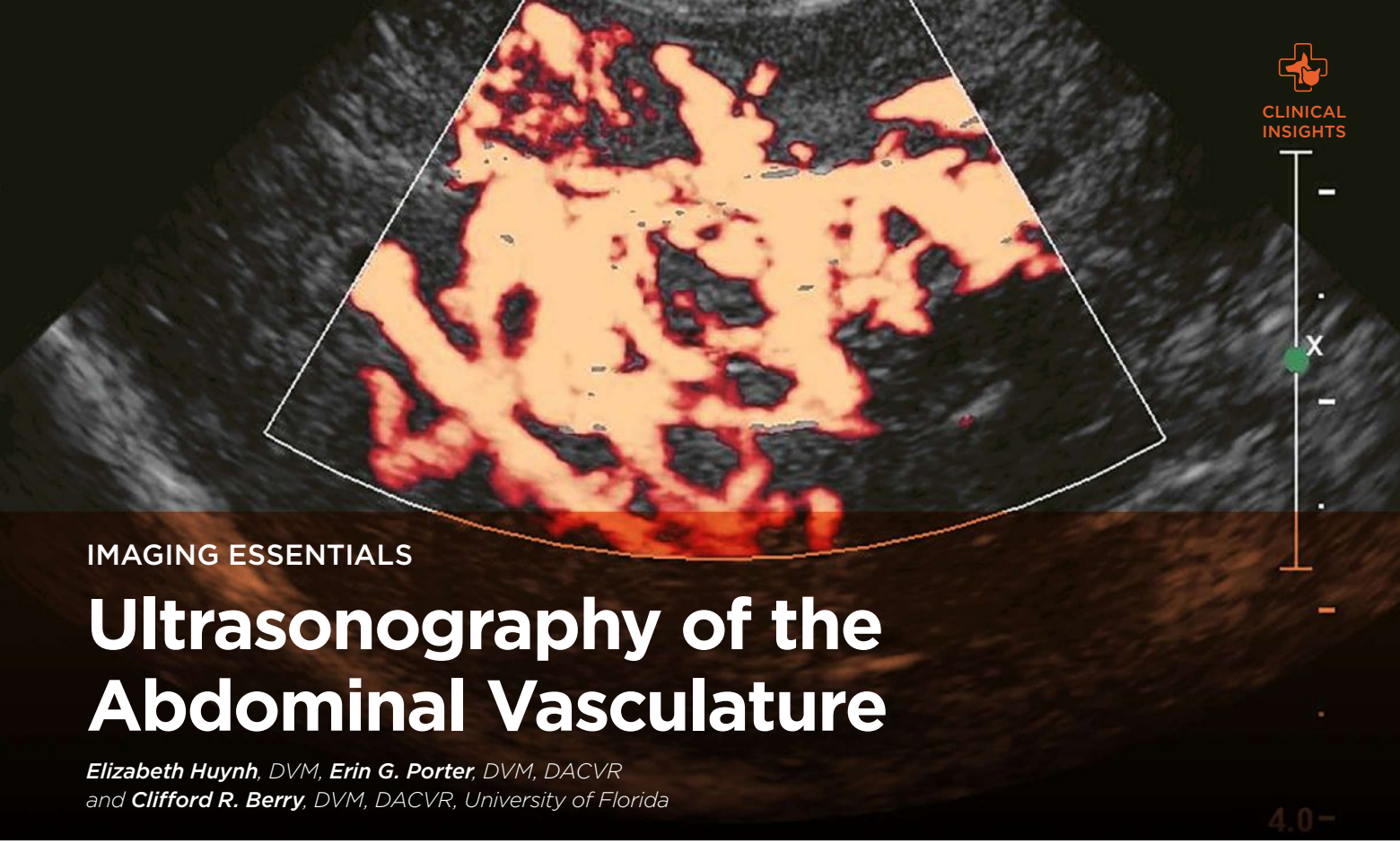

CLINICAL INSIGHTS

IMAGING ESSENTIALS

Ultrasonography of the Abdominal Vasculature

***Elizabeth Huynh**, DVM, **Erin G. Porter**, DVM, DACVR*
*and **Clifford R. Berry**, DVM, DACVR, University of Florida*

Welcome to our series of articles on small animal abdominal ultrasonography. The initial articles provided an overview of basic ultrasonography principles and a discussion about how to perform a systematic scan of the abdomen. The rest of the series discusses ultrasound evaluation of specific abdominal organs/systems. Read the other small animal abdominal ultrasonography articles published in *Today's Veterinary Practice* at todaysveterinarypractice.com.

Indications for imaging the abdominal vasculature include ruling out neoplastic vascular invasion, determining the presence or absence of suspected congenital vascular anomalies, and identifying intravascular thrombi (e.g., in cases of suspected hypercoagulability). The ability to identify abdominal vasculature is also important, as these vessels are used to find normal anatomic structures, such as the pancreas, lymph nodes, and adrenal glands.

Thorough evaluation of the abdominal vasculature and lymph nodes, when identifiable, is part of a complete abdominal ultrasound examination and requires experience as well as an understanding of anatomy and Doppler ultrasonography techniques. For more details on the relationship of the abdominal vessels and lymph nodes, please see the July/August 2017 Imaging Essentials article, "Ultrasonography of Peritoneal and Retroperitoneal Spaces and Abdominal Lymph Nodes," on todaysveterinarypractice.com.

DOPPLER ULTRASONOGRAPHY

Doppler ultrasonography is used to evaluate characteristics of blood flow: its presence or absence, direction, velocity, and character (laminar versus turbulent flow). The 4 Doppler techniques used in ultrasonography are continuous-wave, pulsed-wave, power, and color Doppler, which are divided into spectral displays and color modes. The advantages and disadvantages of the techniques used for abdominal ultrasonography are summarized in **TABLE 1**.[1] The Doppler principle is based on the Doppler shift frequency equation (**FIGURE 1**). The change in frequency is in the kHz range and can be heard when displaying spectral Doppler images.

Imaging Techniques

Spectral Doppler

The image is displayed as blood flow velocity (y axis) as a function of time (x axis). Ideally, the sampling line for spectral Doppler imaging is

PEER REVIEWED

TABLE 1 Comparison of Pulsed-Wave, Color, and Power Doppler[1]

	PULSED-WAVE DOPPLER	COLOR DOPPLER	POWER DOPPLER
Properties	Examines the flow waveform within a specific part of the vessel being interrogated	Provides a map of flow superimposed over an organ or structure	Color brightness is related to the number of moving cells (presence of blood flow)
Advantages	Provides directional information about flow	Provides directional information about flow (BART)	Sensitive: can detect low-flow states in smaller-diameter vessels
	Provides velocity information and allows calculation of specific indices (resistive index in the kidneys, systolic:diastolic ratios, etc.)	Provides velocity information and shows vascular distribution within the organ of interest	Not angle dependent
	Assesses the laminar appearance of blood flow and any flow disturbances	Detects turbulent flow, lack of flow, and high-flow velocities as seen with aliasing	Free from aliasing
Disadvantages	Location only delivered in combination with additional images such as real-time B-mode	Limited by respiratory influence (very difficult to obtain in a panting animal)	No directional information
	Highly angle dependent so that flow perpendicular to the transducer is registered as zero. Should strive to keep all angle-corrected interrogations < 60° in the abdomen.	Angle dependent; flow perpendicular to the transducer is recorded as zero	No velocity information
		Lowers frame rate due to increased computer processing required	No flow character information
		Poor temporal resolution	Susceptible to noise and motion

BART, blue away and red toward the transducer.

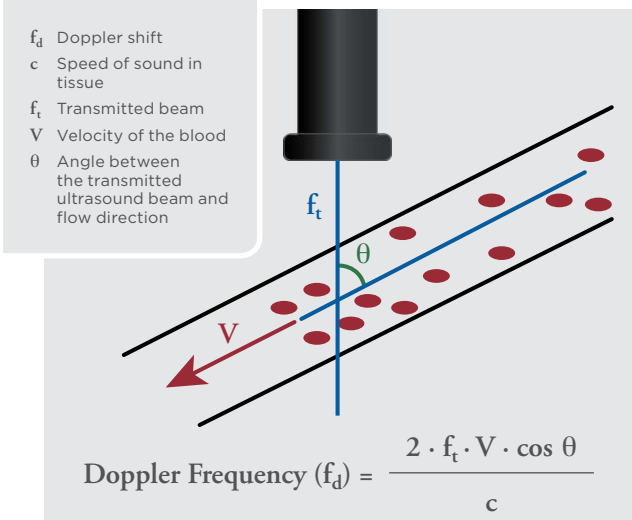

FIGURE 1. Diagram of Doppler ultrasonography and the Doppler shift frequency equation. The Doppler shift (f_d) is measured by the ultrasound machine as the difference between the transmitted (f_t) and reflected ultrasound frequency as a result of the motion of red blood cells. The equation shows that measurement of f_d is related to the velocity (V) of blood flow. The speed of sound (c) in tissue is assumed to be a constant at 1540 m/sec for the purpose of this calculation. Note that the cos 90° is 0; therefore, if the angle of f_t is 90°, the measured blood flow will be 0.

parallel to the area of interest or lines up with the flow of blood so that the angle of incidence of the ultrasound beam is 0°. If the incident angle is 90°, no flow will be displayed (**FIGURE 1**).

Two types of spectral Doppler techniques are used today: continuous wave and pulsed wave.

Continuous-wave Doppler is used in echocardiography. It uses phased array transducers, which contain multiple crystals that independently and continuously transmit and receive ultrasound waves. The advantage of continuous-wave Doppler is that it can record high blood flow velocities (>6 m/sec) with high fidelity (no aliasing artifact; **BOX 1**). It also gives the direction of blood flow relative to the transducer: flow directed toward the transducer is above the baseline (positive direction), and flow away from the transducer is below the baseline (negative direction). Its disadvantage is that flow velocities are recorded along the line of interrogation, and a specific anatomic location along that line is not accurately recorded. This is called *range ambiguity*.

PEER REVIEWED

BOX 1. Aliasing in Spectral Pulsed-Wave Doppler Images

Aliasing in spectral pulsed-wave Doppler images is an artifact that appears as a "wraparound" of the maximum velocities to the opposite side of the pulsed-wave spectral display in the y direction. The maximum velocity (up to 1.5 to 2.0 m/sec) that can be accurately recorded in pulsed-wave Doppler is a function of the sampling frequency, also called the **pulse repetition frequency** (PRF), and the depth of the interrogating sampling volume. For a given PRF, the maximum frequency shift that can be recorded without aliasing is equal to half the PRF. This maximum shift is known as the **Nyquist limit**.

To reduce aliasing, the ultrasonographer may increase the PRF (often called *scale* on ultrasound machines), decrease the baseline, or reduce the depth of the sample volume to allow PRF to increase with the lack of depth constraints. If the PRF is set correctly, aliasing indicates high-velocity and/or turbulent blood flow. The incident angle can be corrected by a sampling gate angle correction; however, an angle above 60° is not recommended.

Pulsed-wave Doppler is used in both echocardiography and abdominal/vascular ultrasonography. In pulsed-wave Doppler, the pulse–echo principle (the same crystal transmits and receives the ultrasound wave) is used to measure blood flow velocity, direction, and pattern (laminar versus turbulent).

The advantage of pulsed-wave Doppler is that the exact anatomic location of the returning velocity can be accurately recorded by specifying where the ultrasound transducer should "listen" for returning echoes along the line of Doppler interrogation. The specified area, known as a *sampling gate*, is displayed as two parallel lines along the interrogation line. There is no range ambiguity.

A disadvantage of pulsed-wave Doppler is that it is limited by aliasing artifact for higher velocities (>2.0 m/sec; **BOX 1**). This clearly affects the utility of pulsed-wave Doppler in echocardiography, where pathologic velocities can easily exceed this limit; however, pulsed-wave Doppler is adequate for vascular evaluation in the abdomen.

When pulsed-wave Doppler is used for abdominal vessels, the angle between the vessel being interrogated and the transducer at the skin's surface will never reach 0°. Therefore, these machines have a dial for angle correction. Angles > 60° result in sampling inaccuracy for peak flow velocity.

Color Display Doppler

In this form of pulse-echo Doppler, the returning frequencies are displayed based on a color display known as BART, in which *blue* indicates flow *away* from the transducer and *red* indicates flow *toward* the transducer. The color spectrum indicates the velocity range or scale, which is displayed on the image, typically on the right.

Color Doppler displays the presence or absence, direction, velocity, and character (laminar versus turbulent) of blood flow. In this technique, the color Doppler button is engaged and a box (sample window) is overlaid on the grayscale image. Within this box, changes in frequency based on the presence of motion in the vessels result in a color display of the velocity for each pixel (**FIGURE 2**). One available color display is called a *variance map*, in which velocities that exceed the pulse repetition frequency are displayed as green

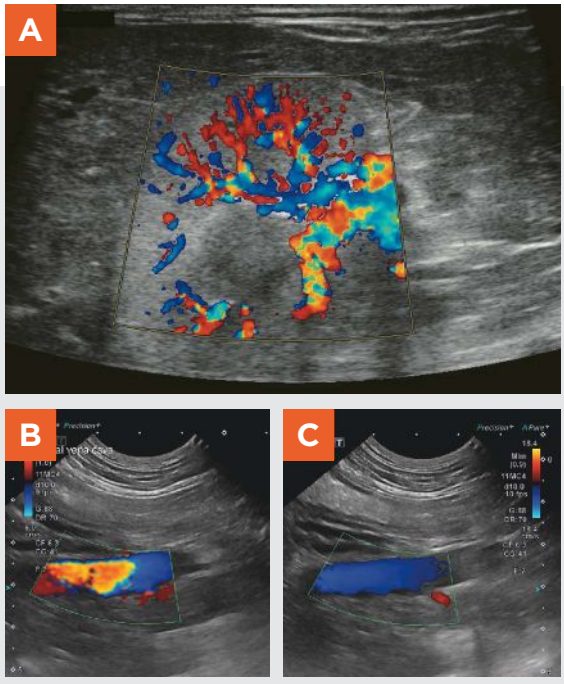

FIGURE 2. (A) Long-axis view of the right kidney in a normal cat using color Doppler. Note the red vessels indicating blood flow toward the transducer and the blue vessels indicating flow away from the transducer. **(B)** Color Doppler image of the caudal vena cava of a dog in dorsal recumbency as imaged from the right side in long axis. Aliasing (red, yellow, and orange) can be seen because the pulse repetition frequency or Doppler scale has been set too low at 6.0 cm/sec. **(C)** The same dog as in B. The Doppler scale has been adjusted correctly to 18.4 cm/sec to eliminate aliasing.

rather than aliasing and wrapping around into the opposite color column.

Power Doppler displays only the presence or absence of blood flow. Some ultrasound units have directional power Doppler imaging in which the presence and direction of flow are recorded. These settings are not as sensitive as power Doppler without the directional information (**FIGURE 3**).

Applications

All normal blood vessels possess certain ultrasonographic features. On grayscale ultrasonographic imaging, the vascular lumen should be anechoic. Slice thickness artifacts may result in spurious echoes within the lumen, but color Doppler interrogation of the vessel in both short- and long-axis planes helps differentiate between artifact and abnormality. When done with the correct machine settings, color Doppler interrogation of the vessels should result in a solid color within the lumen representative of flow in the expected direction toward (red) or away from (blue) the transducer (**FIGURE 2**). It is important to note that, depending on the direction of the blood flow in the vessel relative to the transducer, flow in both arteries and veins may be displayed as red, blue, or both colors in the same vessel. For example, if the transducer is perpendicular to the aorta with the marker of the transducer pointing cranially, the flow in the aorta will be red on the left side of the display window and blue on the right side of the display window.

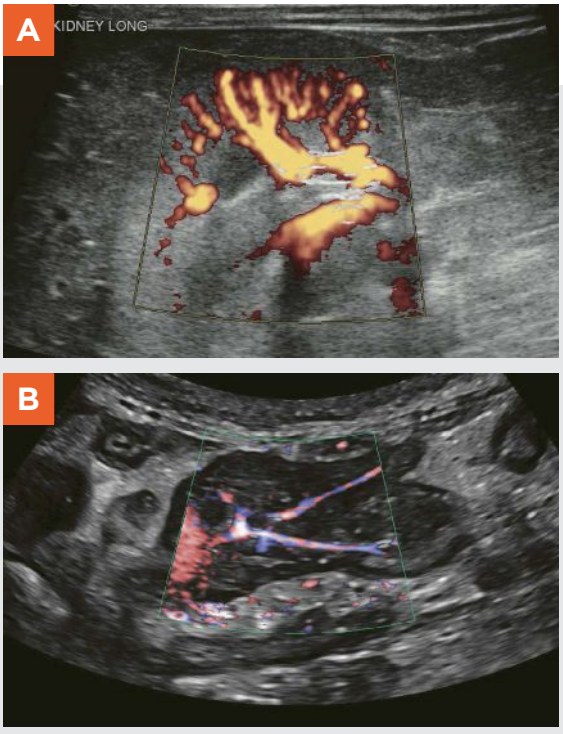

FIGURE 3. (A) Long axis of the right kidney in a normal cat using power Doppler as seen in **FIGURE 2A**. This method detects presence of blood flow but gives no information on the direction, velocity, or turbulence of flow. Note that aliasing is not seen. **(B)** Directional power Doppler from a jejunal lymph node affected with lymphoma in a cat. This image provides directional information as well as the presence or absence of flow. Note the abnormally enlarged and infiltrated lymph node.

PREPARATION AND SCANNING TECHNIQUE

Examination of the abdominal vasculature is part of a comprehensive routine abdominal ultrasound examination. Before beginning the examination, clip the patient's hair and apply ultrasonic gel to the skin. The cranial abdominal organs should be evaluated for their normal vasculature (liver, spleen, and left kidney). The arteries surrounding the left adrenal gland are used to localize this gland. If the ultrasonographer scans the abdominal cavity in a clockwise fashion, the caudal abdominal vasculature examination can be reviewed after examining the urinary bladder and reproductive tract.

Begin by angling the transducer from the left caudodorsal aspect of the left paralumbar space ventral to the hypaxial muscles to image the retroperitoneal cavity in long axis. The aorta and caudal vena cava will be seen dorsal to the urinary bladder and descending colon. When imaged from the left, the aorta will be dorsal and in the near field and the caudal vena cava will be ventral and in the far field.

Next, place the transducer in a similar position on the right side of the patient, again in long axis with the patient and angled toward the retroperitoneal cavity dorsally. This window will show the caudal vena cava in the near field and the aorta in the far field. In addition to using anatomic landmarks to identify the aorta and caudal vena cava, the ultrasonographic and physiologic characteristics of these vessels may be considered: the aorta is pulsatile whereas the caudal vena cava is compressible (flattens easily when pressure is applied with the probe on the overlying abdominal wall).

Complete evaluation of the aorta and caudal vena cava in both long- and short-axis views relative to the patient requires following their course

PEER REVIEWED

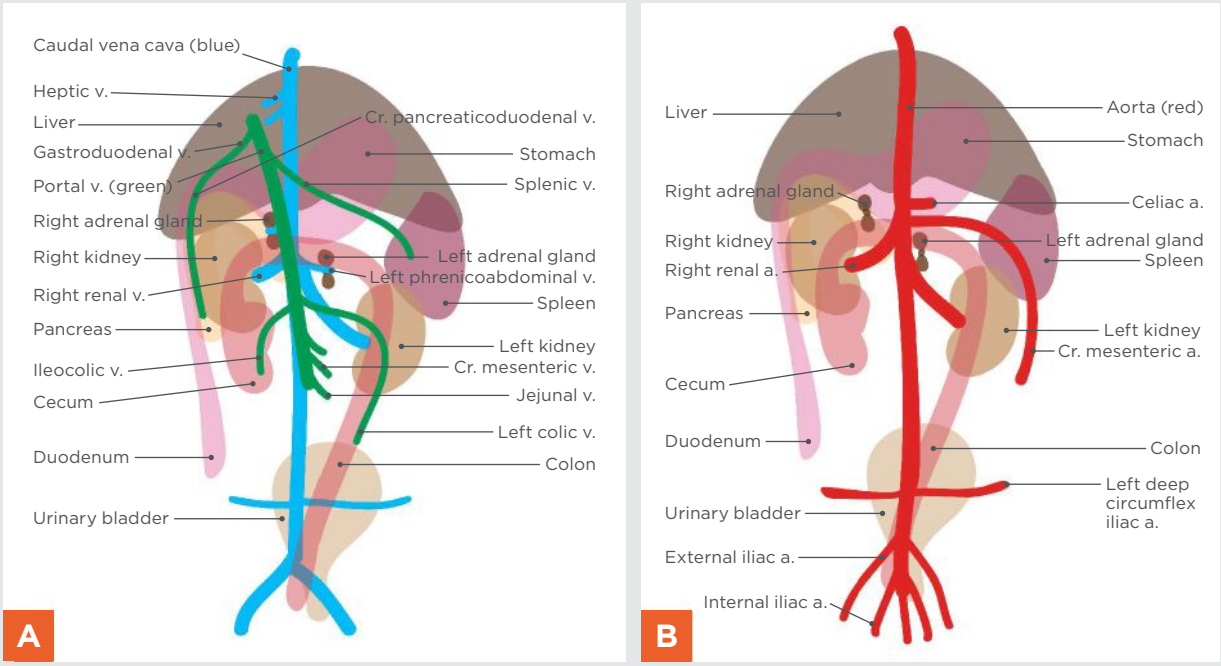

FIGURE 4. (A) Diagram of the portal vein, the caudal vena cava, and their main abdominal branches and tributaries. **(B)** Diagram of the aorta and its main abdominal branches. a, artery; v, vein.

caudally to the trifurcation (origin of the left and right external iliac arteries and continuation of the caudal abdominal aorta) and cranially to the cranial abdominal efferent arteries of the aorta, including the renal arteries and veins, cranial mesenteric artery, and celiac artery (**FIGURE 4**).

NORMAL ULTRASONOGRAPHIC FEATURES OF ABDOMINAL VASCULATURE

On routine abdominal ultrasonography, the aorta, caudal vena cava, portal system, and their branches/tributaries should be visualized (**FIGURE 4**).

Aorta

The aorta is best visualized in the caudodorsal abdomen, just to the left of midline, where it runs parallel to the caudal vena cava (on the right) from the level of L3 to L6. Cranial to L3, the caudal vena cava and the aorta diverge.

The aorta is dorsal to the caudal vena cava throughout the length of the abdomen until the level of L6-L7, where the caudal vena cava and the common iliac veins move dorsal to the aorta and its caudal branches. The cranial mesenteric and celiac arteries can be identified as they leave the aorta cranial to the renal artery; their location is important for identifying the left adrenal gland (**FIGURE 4**). Color Doppler is needed to identify smaller arteries. At the trifurcation of the caudal abdominal aorta, the medial iliac lymph nodes are adjacent to the lateral borders of the aorta and external iliac arteries on the right and left sides.

The aortic diameter can be used as an internal reference to evaluate the renal size in dogs,[2] which is an important parameter in the assessment of canine renal disease. One study indicated that the ratio of left renal length, measured in long-axis plane, and adjacent aortic luminal diameter (LK:Ao) should be between 5.5 and 9.1 in normal dogs.[2]

The aorta should be a straight, anechoic tube with no mineralization within its wall. The walls of the aorta will be discrete hyperechoic lines that do not change diameter until the trifurcation in the caudal abdomen. The normal pulsed-wave Doppler spectral display includes a triphasic spike, with peak velocities reached during ventricular systole. There is a short reversal of flow (signal drops below baseline) followed by a positive rebound from the compliance and elasticity of the ascending aorta and aortic arch (*Windkessel effect*; **FIGURE 5A**). The laminar flow of the blood within the aorta should cause an area relatively void of signal in

Dr. Elizabeth Huynh (2)

the middle of the upward systolic deflection. Normal systolic velocities in the aorta reach 1.0 to 1.5 m/sec.

Caudal Vena Cava

The caudal vena cava can be seen most easily in the abdomen, right of midline, where it runs parallel and adjacent to the aorta in the caudal abdomen, and in the cranial abdomen where it traverses the right side of the liver before crossing the diaphragm. At the level of L3, the caudal vena cava begins its ventral course (away from the aorta and dorsal position in the abdomen) to the level of a mid-diaphragmatic position in the cranial abdomen, as seen on thoracic radiographs.

The cranial aspect of the abdominal caudal vena cava, at the level of the caudate process of the caudate lobe of the liver, is used as a landmark to find the right adrenal gland, as the right adrenal gland is located immediately dorsolateral or lateral to the caudal vena cava at the level of the renal hilum. Cats deposit fat between the caudate lobe of the liver (renal fossa) and the right kidney (located in a more caudal position than in dogs). In cats, the right adrenal gland is located cranial to the right kidney along the lateral border of the caudal vena cava at the level of the liver.

The pulsed-wave Doppler spectral waveform is complex and is influenced by cardiac cycle and the phase of respiration as well as patient motion (**FIGURE 5B**). If imaging the vessel so that blood flow is toward the transducer, there will be an initial positive waveform at the time of ventricular systole. Before the waveform reaches baseline, there will be another positive spike during late diastolic filling as the right ventricular and right atrial pressure increases; during atrial contraction, there will be a negative deflection as blood flows from the right atrium into the right ventricle. Because the flow velocity varies in the caudal vena cava, a laminar flow pattern will not be seen. The peak velocities in the caudal vena cava (at the time of right ventricular systole) are typically around 20 to 35 cm/sec.

Portal Vein

The portal vein has a characteristic flat venous pulsed-wave Doppler profile (**FIGURE 5C**) and is located within the porta hepatis, dorsal to the body of the pancreas. Moving cranially, the portal vein is formed by the confluence of cranial and caudal mesenteric portal veins, the splenic portal veins, and the gastroduodenal portal vein. The portal vein proper is a very short vessel that travels into the porta hepatis and gives off the right divisional branch (right liver lobes) and the central divisional branch (quadrate and central hepatic lobes) and continues on as the left divisional branch (left hepatic lobes). The flow pattern is nonlaminar and the typical flow velocities are 15 to 25 cm/sec.

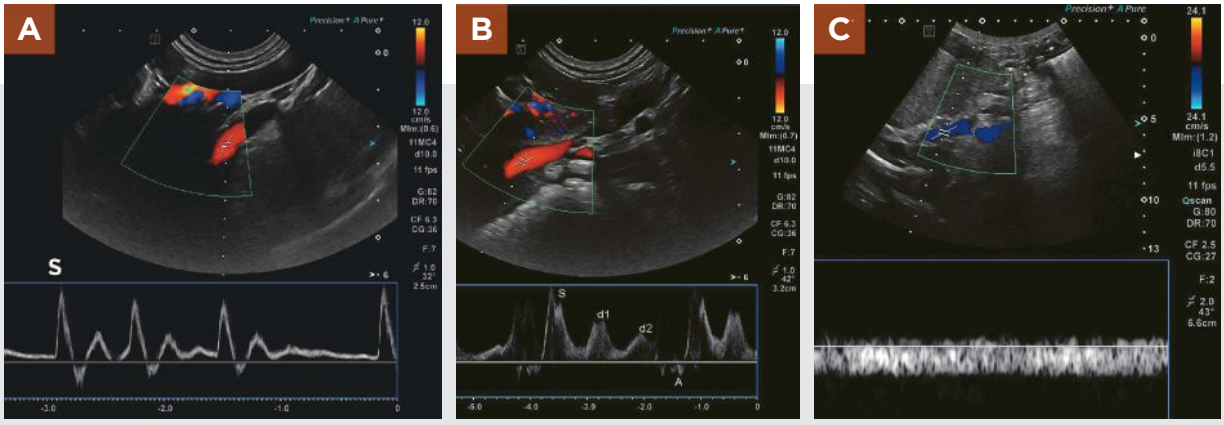

FIGURE 5. Pulsed-wave Doppler evaluation of a 1-year-old mixed-breed dog under sedation (Dexdomitor 0.25 mcg/kg). **(A)** Long-axis view of the abdominal aorta from a right-sided window that documents the typical triphasic appearance of the pulsed-wave Doppler spectral tracing. The peak velocity is typically < 1 m/sec. The dog had a sinus arrhythmia so that after the long diastolic pause, there was a "stronger" systolic contraction (increased stretch of myocardial fibers due to increased ventricular filling; S); the first contraction is taller (higher velocity) than the other 2 beats during inspiration. **(B)** Long-axis view of the caudal vena cava as imaged from the right. Due to the decreased heart rate from the sedation, there are 4 peaks on the pulsed-wave Doppler spectral tracing of the caudal vena cava instead of the standard three. The initial positive deflection (note that the spectral trace has been inverted as the position of the sampling gate; flow would be away from the transducer) represents ventricular systole. The diastolic filling phase has been divided into 2 parts (d1 and d2), and there is flow reversal at atrial contraction **(A)**. **(C)** Long-axis view of the portal vein as imaged from the right. The pulsed-wave Doppler spectral tracing of the portal vein is typical in appearance, with a flat profile and not under the influence of the cardiac cycle or respiration.

PEER REVIEWED

TABLE 2 Selected Thrombotic Risk Factors in Dogs and Cats[1,3–5]

DOGS	CATS
PATIENT DISEASES AND CONDITIONS	
Immune-mediated hemolytic anemia	Immune-mediated hemolytic anemia
Sepsis	Sepsis
Neoplasia[6]	Neoplasia[6]
Cardiovascular disease (eg, cardiomyopathy, heartworm disease)[7,8]	Cardiovascular disease (eg, cardiomyopathy, heartworm disease)[7,8]
Pancreatitis	Pancreatitis
Glomerular disease (protein-losing nephropathy)[9]	Glomerular disease (protein-losing nephropathy)[9]
Cardiac disease (eg, endocarditis[10])	Protein-losing enteropathy
Hyperadrenocorticism (Cushing's disease or syndrome)	Hepatic lipidosis
Disseminated intravascular coagulopathy[9]	Feline infectious peritonitis
Amyloidosis	Pneumonia
Hypothyroidism	Encephalitis
Blastomycosis[11]	Steroid administration
Trauma	
TREATMENTS	
Intravenous catheter placement	Steroid administration
Recent surgery	
Cytotoxic drugs	
Blood transfusion	
Total hip implant	

VASCULAR ABNORMALITIES

Thromboembolic Disease

Thromboembolic disease can affect any of the intraabdominal vessels and is caused by a hypercoagulable state (**TABLE 2**).[1,3–11]

Ultrasonographically, chronic thrombi appear as echogenic tissue within the lumen of the vessel, causing partial or a complete obstruction of visualized blood flow (**FIGURE 6**). Acutely, thrombi can be difficult to visualize as they are anechoic. If thrombi are suspected, color, power, and pulsed-wave Doppler interrogation is recommended, and any lesion should be confirmed by imaging in both long- and short-axis planes.

Animals presenting in a hypercoagulable state may have slow blood flow that can be recognized before thrombus formation. On grayscale images, this can appear as echogenic "smoke" within the vessels, which is likely due to spontaneous agglutination of erythrocytes that increases the blood backscatter and echogenicity.

Thorough evaluation of thromboembolism includes assessment for the following[12]:

1. Acute thrombi (using color and pulsed-wave Doppler)
2. Extent and location of visible thrombi (using color Doppler for evaluation of collateral circulation)
3. Peripheral blood flow (using color Doppler)
4. Evidence of neoplasia in the region
5. Sequelae of thrombosis (e.g., ischemia of distal structures/organs, evaluated using color Doppler; ascites from portal vein thrombosis)

Vascular anomalies other than those arising from the portal system are rare. Other imaging modalities, such as, computed tomographic angiography are usually required for definitive diagnosis.

Caudal Vena Cava Thrombosis

Caudal vena cava abnormalities are most commonly associated with neoplasia of the right adrenal gland, but can occur secondary to invasion by left adrenal, hepatic, lymph node, or renal neoplasia or from extension of femoral or iliac venous thrombosis. It is difficult to differentiate between thromboses that are blood clots and those that represent true tumor thrombi. Both blood clots and tumor thrombi appear as echogenic structures within the lumen of the vessel. Color Doppler imaging shows a filling defect within the vessel (**FIGURE 6**). Complete occlusion results in absence of flow beyond the lesion. Partial occlusion may result in turbulence adjacent to the lesion or aliasing. However, if the tumor is vascular, a flow pattern may be visible within the thrombus, particularly when using power Doppler. This finding would be consistent with a tumor thrombus.

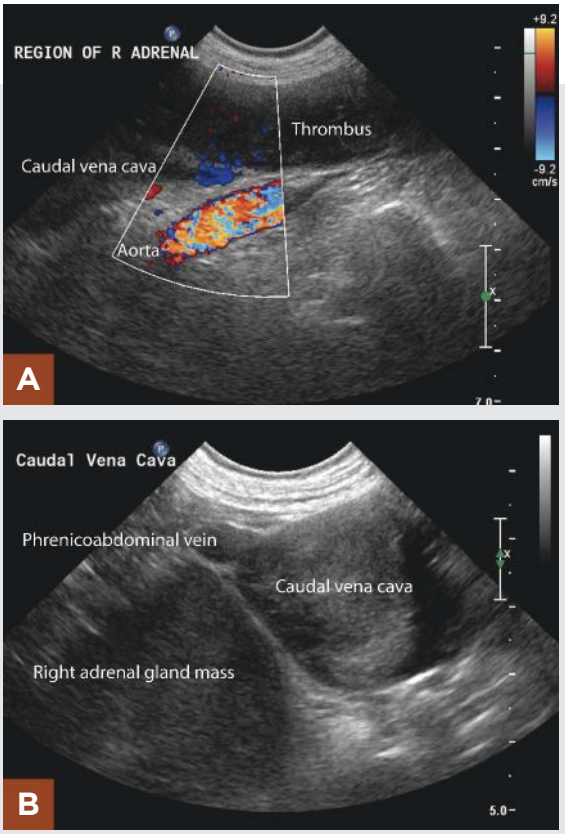

FIGURE 6. (A) Long-axis and **(B)** short-axis views of the caudal vena cava at the level of the right adrenal gland in a dog with a pheochromocytoma invading the adjacent vena cava. In A, note the formed echogenic structure filling much of the caudal vena caval lumen, causing little flow in the far field of the caudal vena cava when investigated with color Doppler. In B, the formed echogenic thrombus fills most of the caudal vena cava (semilunar anechoic structure) and part of the adjacent phrenicoabdominal vein. A hypoechoic right adrenal gland mass is also present.

Portal Vein Thrombosis

Thrombosis of the portal vein occurs with numerous diseases associated with the development of coagulopathies.[2,13] It is recognized ultrasonographically as intraluminal structures of moderate to high echogenicity and the absence of color Doppler signals within the lumen[14] (**FIGURE 7**). Thrombosis can be focal or can extend into all branches of the portal venous system, resulting in secondary portal venous hypertension, acquired extrahepatic portosystemic shunts (PSSs), and ascites.

Aortoiliac Thrombosis

Aortic and iliac arterial thromboembolism is most commonly seen in cats with primary cardiomyopathy; in dogs, it may be secondary to neoplasia, cardiac disease, or hypercoagulable states. The ultrasonographic features are similar to those of a venous thrombus.

Hepatic Venous Congestion

Congestion usually occurs secondary to increased resistance to blood flow of the caudal vena cava to the right atrium. Causes of hepatic venous congestion include obstruction by a right atrial mass, pericardial effusion, invasion of the caudal vena cava by a tumor, and right-sided congestive heart failure.[15] Distention of the hepatic veins and caudal vena cava is best visualized adjacent to the diaphragm at the level of the right cranial dorsal abdomen (10th or 11th intercostal space approach). Concurrent findings include a diffusely hypoechoic hepatic parenchyma, hepatomegaly, and peritoneal effusion.

Portosystemic Shunts

Congenital Portosystemic Shunts

Congenital PSSs are single, large, anomalous connections between the portal and systemic veins that allow portal blood from the gastrointestinal tract to bypass the liver. Congenital PSSs are more frequently

PEER REVIEWED

Congenital PSSs are single, large, anomalous connections between the portal and systemic veins that allow portal blood from the gastrointestinal tract to bypass the liver.

seen in dogs than in cats. A congenital shunt can be intrahepatic or extrahepatic. A complete description and review of this material are beyond the scope of this article, so only the essentials are discussed here.

Intrahepatic congenital PSSs occur predominantly in large-breed dogs and are often attributable to a patent ductus venosus, originating from the intrahepatic left division of the portal vein and connecting to the left hepatic vein.[16,17] If originating from the right branch of the portal vein, these shunts drain directly into the caudal vena cava.

Extrahepatic congenital PSSs in dogs are connections between the portal system (either the portal vein or any of its afferents, such as the left gastric vein, splenic vein, or gastroduodenal vein) and the systemic venous circulation (either the caudal vena cava or the azygos vein).

Cats may have intrahepatic or extrahepatic shunts; the morphology of extrahepatic shunts varies widely depending on their origin, course, and termination.[18,19]

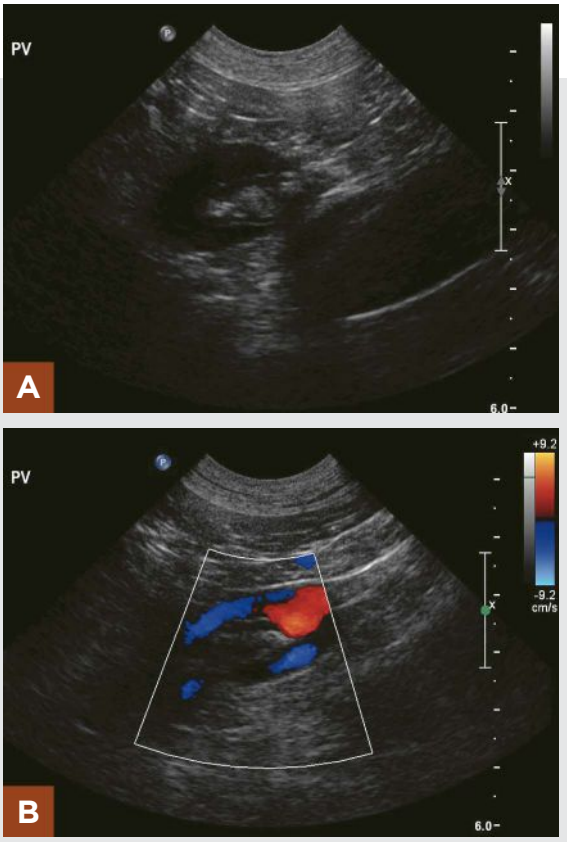

FIGURE 7. Short-axis view of the portal vein, represented by the anechoic structure in the near field, and caudal vena cava, represented by the anechoic structure in the far field, at the level of the porta hepatis in an adult dog with hypercoagulopathy **(A)**. Note the ovoid, echogenic structure in the lumen of the portal vein **(A)** and the disrupted color flow Doppler signal with a filling defect within the lumen corresponding to a portal vein thrombus **(B)**.

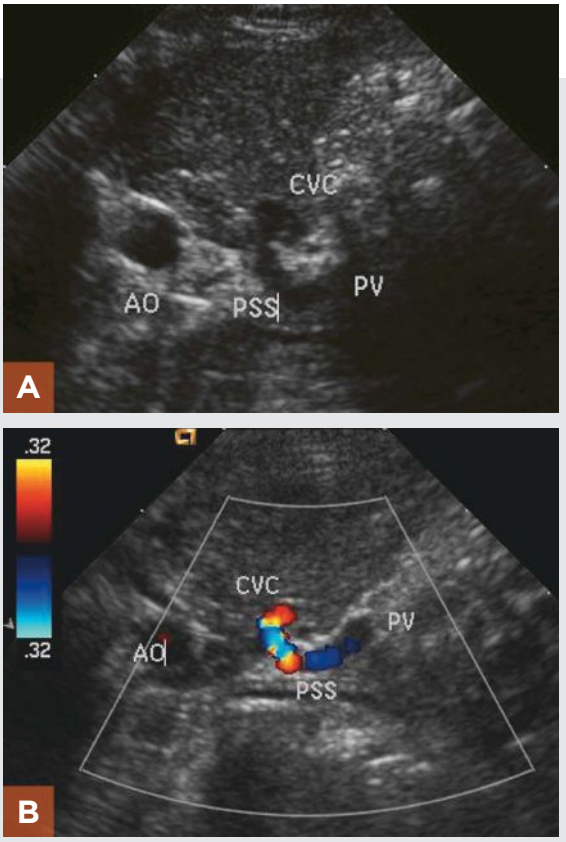

FIGURE 8. Short-axis view of the liver **(A)** without and **(B)** with color Doppler at the level of the portal vein and caudal vena cava in a 2-month-old mixed-breed puppy with a portocaval intrahepatic shunt. Note the turbulent blood flow, denoted by the aliasing artifact, in the lumen of the anomalous shunting vessel and the portal vein. This turbulence is consistent with an extrahepatic portocaval shunt.

Extrahepatic portocaval shunts typically originate from the splenic, right gastric, or left gastric vein and enter the caudal vena cava between the phrenicoabdominal vein and the diaphragm. They are usually identified as a tortuous vessel with hepatofugal flow as noted using color or pulsed-wave Doppler. *Hepatofugal flow* is flow within the portal vein or one of its afferents that is directed away from the liver, contrary to normal dogs and cats, in which the portal vein flows toward the liver (hepatopetal flow). The vena cava, portal vein, and porta hepatis region should be scanned from the diaphragm to the level of the kidneys in search of an anomalous branching vessel entering the vena cava or travelling dorsally through the diaphragm toward the azygous vein adjacent to the aorta. The point of entry of portocaval shunts into the caudal vena cava can be identified by recognition of turbulent flow with color and pulsed-wave Doppler (**FIGURE 8**).

Acoustic windows include the subxiphoid and right caudal intercostal spaces of the last 3 ribs, relatively close to the spine, where the liver is visualized cranial to the right kidney. Using these intercostal windows, the ultrasonographer can image in short axis the adjacent aorta, caudal vena cava, and portal vein (**FIGURE 9**). The shunting vessel can be identified coursing between the vena cava and portal vein (**FIGURE 8**). Portal vein size can also be measured in the 12th or 11th dorsal intercostal window. The size of the portal vein cranial to the shunt is generally reduced in diameter. When the portal vein is measured cranial to the gastroduodenal-portal confluence, a portal vein: aortic diameter ratio of ≤ 0.65 is predictive for the presence of an extrahepatic shunt, and a value of ≥ 0.80 excludes it (**FIGURE 9**).[20] If the ratio is ≥ 0.80, other types of disease, such as microvascular dysplasia, intrahepatic shunt (**FIGURE 10**), and portal hypertension attributable to chronic liver disease with a secondary extrahepatic PSS, could still be present.

The sensitivity and specificity of ultrasonography for the detection of extrahepatic PSSs have been reported to be 80.5% and 66.7%, respectively; a greater sensitivity of 100% was seen for intrahepatic PSSs alone.[21] In addition, microhepatia, bilateral renomegaly, nephrocalcinosis, nephroliths, and cystoliths attributable to urate crystals[22,23] or stones may be identified.[24]

Acquired Portosystemic Shunts

Multiple acquired extrahepatic PSSs develop secondary to chronic portal hypertension and result in reduced

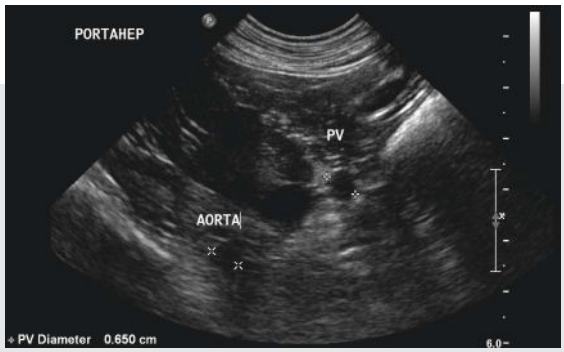

FIGURE 9. Short-axis view of the portal vein and aorta in the region of the porta hepatis in a dog. The portal vein:aortic diameter ratio is 0.84, which indicates that this dog likely does not have an anomalous extrahepatic portosystemic shunt.

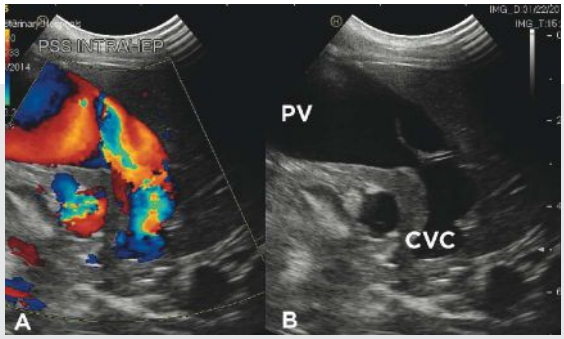

FIGURE 10. Short-axis view of the left division of the liver in a 5-month-old golden retriever with a single intrahepatic portosystemic shunt **(A)** with and **(B)** without color Doppler. Note the cystic, rounded, anechoic structure representing the portal vein (PV) in the left of the image. A large, distended vessel connects with the caudal vena cava. Aliasing and turbulence can be seen in the portal vein, shunt vessel, and caudal vena cava in **A**.

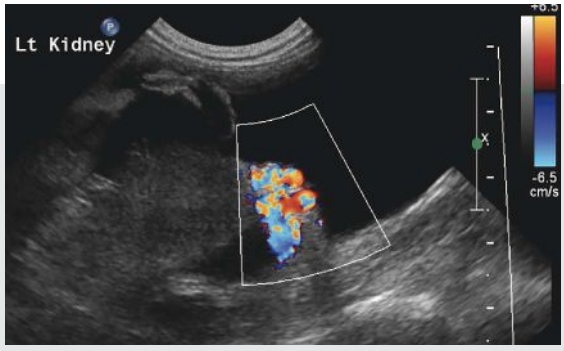

FIGURE 11. Long-axis view (2-dimensional with color Doppler overlay) of the left abdomen near the left kidney at the level of the aorta and caudal vena cava in an 8-year-old poodle with multiple extrahepatic portosystemic shunts (colored circular vessels) secondary to hepatic cirrhosis from sago palm toxicity.

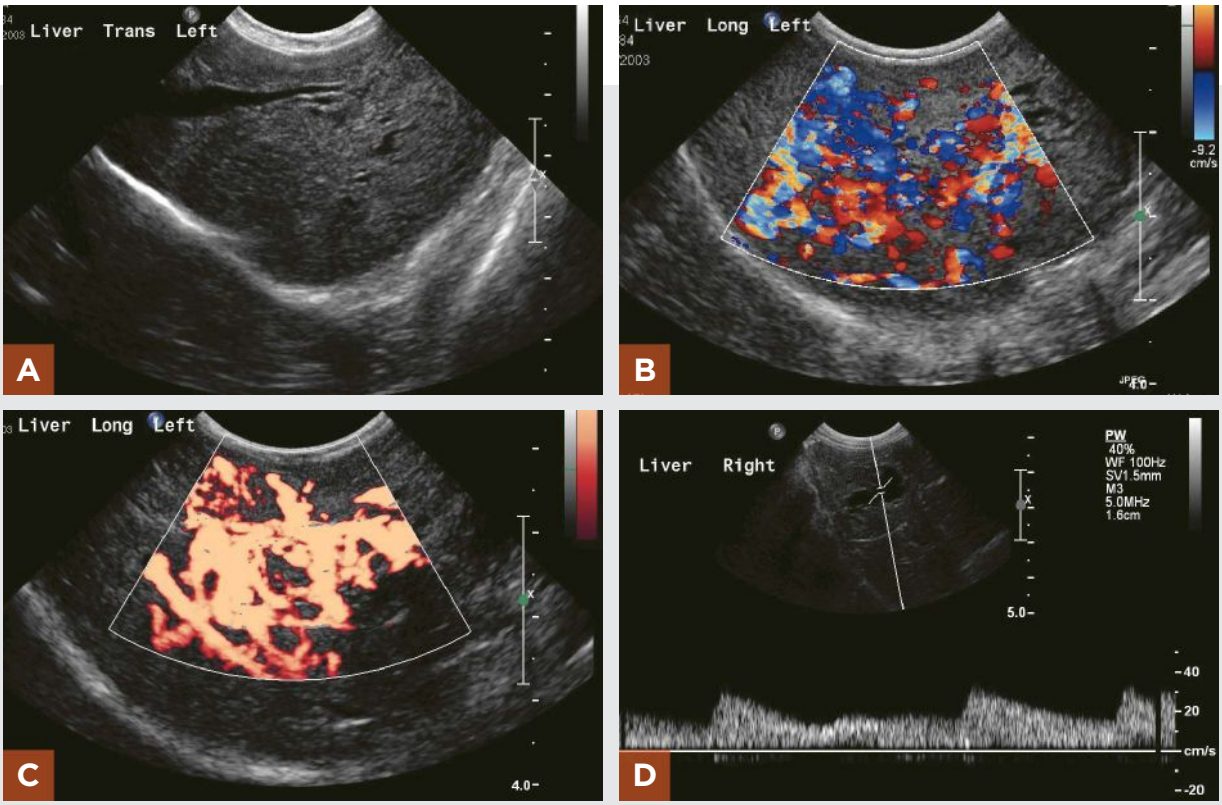

FIGURE 12. Short-axis view of the left division of the liver in a 6-year-old poodle with multiple hepatic arteriovenous fistulas **(A)** without color Doppler, **(B)** with color Doppler, and **(C)** with power Doppler. Note the tortuous spectrum of vessels on the color and power Doppler images, not seen on the 2-dimensional grayscale image. **(D)** The pulsed-wave Doppler display from any of the vessels imaged is seen as a continuous flow pattern with an arterial spike and the lack of return to baseline, consistent with arteriovenous fistula.

blood flow to the liver. Causes of portal hypertension include chronic liver disease with fibrosis, cirrhosis, some forms of infiltrative neoplasia, congenital hypoplasia of the portal vein, hepatic arteriovenous fistula, portal vein thrombosis, and extraluminal portal vein compression. The most common causes of portal hypertension in dogs are disorders causing right-sided heart failure[15,25–27] and severe diffuse hepatobiliary disease,[28] resulting in cirrhosis.

On ultrasonography, acquired extrahepatic PSSs are recognized as multiple small, collateral, tortuous vessels connecting the portal vein or its tributaries to the caudal vena cava and/or renal/gonadal vein, mesenteric and colonic veins, leading to clinical signs of PSS (**FIGURE 11**). Ascites is commonly found in association with portal hypertension, with reduced main portal vein blood flow to mean velocities of ≤ 10 cm/sec as measured on spectral Doppler ultrasonography.[29]

Hepatic Arteriovenous Fistula

Hepatic arteriovenous malformations (fistulas) can be congenital or, less commonly, acquired. They connect the hepatic arteries and portal veins. The surge of high-pressure arterial blood into the low-pressure intrahepatic portal system causes development of severe portal hypertension. These animals usually present at a young age with severe ascites.[30,31]

Ultrasonographically, severe enlargement of the intrahepatic portal branches and main portal vein is seen (**FIGURE 12**). Doppler interrogation of these dilated branches shows turbulent pulsatile flow, indicating communication with the arterial system (**FIGURE 12**). Scanning caudal to the liver, especially in the area of the left renal and gonadal veins, often allows identification of numerous small, tortuous vessels corresponding to acquired PSSs.

SUMMARY

A working knowledge of the abdominal vascular anatomy is required for localization of small structures and for evaluation of the primary abnormalities of the

PEER REVIEWED

aorta, caudal vena cava, and portal vein systems. Systematic evaluation using color, power, and pulsed-wave Doppler interrogation of the various organs and/or vessels requires time and patience. As with normal echogenicity and echotexture of the abdominal organs, the normal color, power, and pulsed-wave Doppler flow patterns should be recognized by the ultrasonographer. TVP

References

1. Gorgas D. Physical principles. In: Barr F, Gaschen F, eds. *BSAVA Manual of Canine and Feline Ultrasonography*. Quedgeley: British Small Animal Veterinary Association; 2012:1-14.
2. Mareschal A, d'Anjou MA, Moreau M, et al. Ultrasonographic measurement of kidney-to-aorta ratio as a method of estimating renal size in dogs. *Vet Radiol Ultrasound* 2007;48:434-438.
3. Mattoon J, Nyland T. *Textbook of Small Animal Veterinary Ultrasound*. 3rd ed. St. Louis: Elsevier Saunders; 2015.
4. Llabres-Diaz F. *Abdominal Vessels*. Gloucester: British Small Animal Veterinary Association; 2009.
5. Dennis R, Kirberger RM, Barr F, et al. *Differential Diagnosis in Small Animal Radiology*. 2nd ed: Elsevier Limited; 2010.
6. Chun R, Jakovljevic S, Morrison WB, et al. Apocrine gland adenocarcinoma and pheochromocytoma in a cat. *JAAHA* 1997;33(1):33-36.
7. Frank JR, Nutter FB, Kyles AE, et al. Systemic arterial dirofilariasis in five dogs. *J Vet Intern Med* 1997;11(3):189-194.
8. Welles EG, Boudreaux MK, Crager CS, et al. Platelet function and antithrombin, plasminogen, and fibrinolytic activities in cats with heart disease. *Am J Vet Res* 1994;55(5):619-627.
9. Ritt MG, Rogers KS, Thomas JS. Nephrotic syndrome resulting in thromboembolic disease and disseminated intravascular coagulation in a dog. *JAAHA* 1997;33(5):385-391.
10. Sykes JE, Kittleson MD, Chomel BB, et al. Clinicopathologic findings and outcome in dogs with infective endocarditis: 71 cases (1992-2005). *JAVMA* 2006;228(11):1735-1747.
11. Ware WA, Fenner WR. Arterial thromboembolic disease in a dog with blastomycosis localized in a hilar lymph node. *JAVMA* 1988;193(7):847-849.
12. Zwingenberger A. Ultrasound of arterial and venous thrombosis. 2007. veterinaryradiology.net/341/ultrasound-of-arterial-and-venous-thrombosis/. Accessed January 2018.
13. Respess M, O'Toole TE, Taeymans O, et al. Portal vein thrombosis in 33 dogs: 1998-2011. *J Vet Intern Med* 2012;26(2):230-237.
14. Lamb CR, Burton CA, Carlisle CH. Doppler measurement of hepatic arterial flow in dogs: technique and preliminary findings. *Vet Radiol Ultrasound* 1999;40(1):77-81.
15. Edwards DF, Bahr RJ, Suter PF, et al. Portal hypertension secondary to a right atrial tumor in a dog. *JAVMA* 1978;173(6):750-755.
16. White RN, Burton CA. Anatomy of the patent ductus venosus in the cat. *J Feline Med Surg* 2001;3(4):229-233.
17. White RN, Burton CA. Anatomy of the patent ductus venosus in the dog. *Vet Rec* 2000;146(15):425-429.
18. Ruland K, Fischer A, Reese S, et al. Portosystemic shunts in cats—evaluation of six cases and a review of the literature. *Berl Munch Tierarztl Wochenschr* 2009;122(5-6):211-218.
19. Lamb CR, Forster-van Hijfte MA, White RN, et al. Ultrasonographic diagnosis of congenital portosystemic shunt in 14 cats. *J Small Anim Pract* 1996;37(5):205-209.
20. d'Anjou MA, Penninck D, Cornejo L, et al. Ultrasonographic diagnosis of portosystemic shunting in dogs and cats. *Vet Radiol Ultrasound* 2004;45(5):424-437.
21. Holt DE, Schelling CG, Saunders HM, et al. Correlation of ultrasonographic findings with surgical, portographic, and necropsy findings in dogs and cats with portosystemic shunts: 63 cases (1987-1993). *JAVMA* 1995;207(9):1190-1193.
22. Dear JD, Shiraki R, Ruby AL, et al. Feline urate urolithiasis: a retrospective study of 159 cases. *J Feline Med Surg* 2011;13(10):725-732.
23. G Caporali EH, Phillips H, Underwood L, et al. Risk factors for urolithiasis in dogs with congenital extrahepatic portosystemic shunts: 95 cases (1999-2013). *JAVMA* 2015;246(5):530-536.
24. Boothe HW, Howe LM, Edwards JF, et al. Multiple extrahepatic portosystemic shunts in dogs: 30 cases (1981-1993). *JAVMA* 1996;208(11):1849-1854.
25. Calvert CA, Thrall DE. Treatment of canine heartworm disease coexisting with right-side heart failure. *JAVMA* 1982;180(10):1201-1203.
26. Berg RJ, Wingfield WE, Hoopes PJ. Idiopathic hemorrhagic pericardial effusion in eight dogs. *JAVMA* 1984;185(9):988-992.
27. Fingland RB, Bonagura JD, Myer CW. Pulmonic stenosis in the dog: 29 cases (1975-1984). *JAVMA* 1986;189(2):218-226.
28. Twedt DC. Cirrhosis: a consequence of chronic liver disease. *Vet Clin North Am Small Anim Pract* 1985;15(1):151-176.
29. Bunch SE, Johnson SE, Cullen JM. Idiopathic noncirrhotic portal hypertension in dogs: 33 cases (1982-1998). *JAVMA* 2001;218(3):392-399.
30. Szatmari V, Nemeth T, Kotai I, et al. Doppler ultrasonographic diagnosis and anatomy of congenital intrahepatic arterioportal fistula in a puppy. *Vet Radiol Ultrasound* 2000;41(3):284-286.
31. Schermerhorn T, Center SA, Dykes NL, et al. Suspected microscopic hepatic arteriovenous fistulae in a young dog. *JAVMA* 1997;211(1):70-74.

Elizabeth Huynh

Elizabeth Huynh, DVM, is a diagnostic imaging resident and graduate student at University of Florida College of Veterinary Medicine. Her interests include ultrasonography, cross-sectional imaging, and nuclear medicine. She received her DVM from Ross University, finished her clinical year at Ohio State University, and completed a diagnostic imaging internship at Animal Specialty and Emergency Center in Los Angeles, California.

Erin G. Porter

Dr. Porter is a 2007 graduate of the University of Florida, College of Veterinary Medicine. Upon graduation, she worked as an equine ambulatory practitioner in the Orlando area for two years before returning to the University of Florida for an equine lameness and imaging internship. Dr. Porter completed a residency In Diagnostic Imaging at the University of Florida and became a diplomat of the American College of Veterinary Radiology in 2013. She has been a clinical assistant professor of diagnostic imaging at the University of Florida since 2013. Her interests include equine orthopedic imaging and small animal ultrasound. She currently lives in Alachua, FL with her husband (Michael) and two young children.

Clifford R. Berry

Clifford R. Berry, DVM, DACVR, is a professor of diagnostic imaging at University of Florida College of Veterinary Medicine. His research interests include cross-sectional imaging of the thorax, nuclear medicine, and biomedical applications of imaging. He received his DVM from University of Florida and completed a radiology residency at University of California–Davis.